EARTH SURFACE PROCESSES AND LANDFORMS
Earth Surf. Process. Landforms **44**, 672–678 (2019)

Published online 14 November 2018 in Wiley Online Library
(wileyonlinelibrary.com) DOI: 10.1002/esp.4536

Letters to ESEX

On the development of a magnetic susceptibility-based tracer for aeolian sediment transport research

Sujith Ravi,[1]* Howell B. Gonzales,[1] Ilya V. Buynevich,[1] Junran Li,[2] Joel B. Sankey,[3] David Dukes[1] and Guan Wang[2]

[1] Department of Earth and Environmental Science, Temple University, 1901 N. 13th Street, Philadelphia, PA 19122, USA
[2] Department of Geosciences, The University of Tulsa, Tulsa, OK 74104, USA
[3] US Geological Survey, Southwest Biological Science Center, Grand Canyon Monitoring and Research Center, Flagstaff, AZ 86001, USA

Received 6 August 2018; Revised 9 October 2018; Accepted 9 October 2018

*Correspondence to: S. Ravi, Department of Earth and Environmental Science, Temple University, 1901 N. 13th Street, Philadelphia, PA 19122, USA. E-mail: sravi@temple.edu

ESPL
Earth Surface Processes and Landforms

ABSTRACT: Aeolian processes – the erosion, transport, and deposition of sediment by wind – play important geomorphological and ecological roles in drylands. These processes are known to impact the spatial patterns of soil, nutrients, plant-available water, and vegetation in many dryland ecosystems. Tracers, such as rare earth elements and stable isotopes have been successfully used to quantify the transport and redistribution of sediment by aeolian processes in these ecosystems. However, many of the existing tracer techniques are labor-intensive and cost-prohibitive, and hence simpler alternative approaches are needed to track aeolian redistribution of sediments. To address this methodological gap, we test the applicability of a novel metal tracer-based methodology for estimating post-fire aeolian sediment redistribution, using spatio-temporal measurements of low-field magnetic susceptibility (MS). We applied magnetic metal tracers on soil microsites beneath shrub vegetation in recently burned and in control treatments in a heterogeneous landscape in the Chihuahuan desert (New Mexico, USA). Our results indicate a spatially homogeneous distribution of the magnetic tracers on the landscape after post-burn wind erosion events. MS decreased after wind erosion events on the burned shrub microsites, indicating that these areas functioned as sediment sources following the wildfire, whereas they are known to be sediment sinks in the undisturbed (e.g. not recently burned) ecosystem. This experiment represents the first step toward the development of a cost-effective and non-destructive tracer-based approach to estimate the transport and redistribution of sediment by aeolian processes. © 2018 John Wiley & Sons, Ltd.

KEYWORDS: sediment tracers; magnetic susceptibility; wind erosion; aeolian processes

Introduction

Aeolian processes, including erosion, transport, and deposition of sediment by wind, are important drivers in earth systems and important feedbacks are known to exist between aeolian processes and vegetation dynamics (Field *et al.,* 2010; Ravi *et al.,* 2011). Even though aeolian processes are natural geomorphic processes in the landscape, climatic shifts and anthropogenic activities can accelerate wind erosion, with profound ramifications for soil and vegetation degradation (Kok *et al.,* 2012; Sharratt *et al.,* 2015; Van Pelt *et al.,* 2017; Webb and Pierre, 2018). Erosion occurs when the wind shear at the soil surface exceeds the shear strength of the soil aggregates (Bagnold, 1941). Non-erodible roughness elements such as vegetation can decrease erosion by absorbing a fraction of the wind momentum (Gillette and Stockton, 1989; Okin and Gillette, 2001). Wind erosion is especially prevalent in many arid and semi-arid regions of the world, which are characterized by patchy vegetation cover. Hence the type and distribution of vegetation cover in arid and semi-arid regions exert an important control on the erosion and transport of sediment by wind (Okin and Gillette, 2001; Breshears *et al.,* 2003; Gonzales *et al.,* 2018).

Disturbances to dryland vegetation such as wildfires can greatly enhance the rates and patterns of soil erosion by wind (Whicker *et al.,* 2002; Sankey *et al.,* 2009; Miller *et al.,* 2012; Ravi *et al.,* 2012; Wagenbrenner *et al.,* 2013). Fires alter the sediment transport dynamics through both the removal of vegetation and through the development of hydrophobicity on the soil surface due to high temperatures (Debano, 2000; Ravi *et al.,* 2009a). Recent studies have shown that the effect of fire on wind erosion occurs at the scale of vegetated microsites in the landscape (Ravi *et al.,* 2009b; Sankey *et al.,* 2012a, 2012b, 2012c; Dukes *et al.,* 2018). These studies show that the microsites that normally act as sediment sinks may

transform into sediment sources after fire. The post-fire redistribution of soil resources is an important control on how grass and shrub vegetation recovers following such a disturbance (Ravi *et al.,* 2009b; Wang *et al.,* 2018).

The aeolian transport and redistribution of sediment from sources to sinks in burned and unburned shrub and grasslands have been successfully quantified using tracer-based approaches (Wang *et al.,* 2017; Dukes *et al.,* 2018). Recently, Dukes *et al.* (2018) used rare earth element (REE) tracers to demonstrate that shrub-vegetated microsites can transform into aeolian sediment sources following a prescribed fire in a shrub-grass transition zone in the northern Chihuahuan desert (New Mexico, USA). However, existing tracer techniques, such as the use of REE oxides are expensive, and the tracer preparation, application, and laboratory analysis (e.g. inductively coupled plasma mass spectrometry; ICP-MS) are labor-intensive (Dukes *et al.,* 2018; Van Pelt *et al.,* 2018). To this end, simpler and cheaper alternative approaches would be useful to assess and quantify the aeolian redistribution of sediment for ecological experiments. A potential method to explore is tracking the spatial changes in low-field magnetic susceptibility (MS) of metal tracers – such as iron-based powders – applied on target areas or microsites in the landscape. Magnetic susceptibility determination has been widely used in various studies as an index for past climate (An *et al.,* 1991), an indicator for environmental pollution (Bityukova *et al.,* 1999; Boyko *et al.,* 2004), for mapping of roadside pollution (Hoffmann *et al.,* 1999), for mapping of heavy-metal contamination in soils (Hanesch and Scholger, 2002), for estimating anthropogenic and lithogenic contributions to minerals in topsoil (Magiera *et al.,* 2006), and for assessment of heavy-mineral content (Buynevich *et al.,* 2007; Pupienis *et al.,* 2013).

The MS properties of applied tracers may offer potential advantages including fast, inexpensive measurements, as well as non-destructive fingerprinting and tracking of sediment movement in the landscape. However, developing an ideal metal tracer to mimic soil movement can be challenging, as the greater density of the metal-tracer powders compared with the natural soil grains may impact their detachment, entrainment, and transport. Hence, the fundamental assumption of the simultaneous depletion of tracer and soil during erosion events may not be valid. We investigated the applicability of a novel cost-effective metal tracer-based methodology for quantifying post-fire aeolian redistribution of iron powder tracers initially applied to the vegetated microsites, using spatio-temporal measurements of magnetic susceptibility.

Methods

Study site

Field experiments were conducted in a shrub–grass transition zone at the Sevilleta National Wildlife Refuge (SNWR) in New Mexico, USA. Predominant plants at the field site include black grama grasses (*Bouteloua eriopoda*) and creosote bush shrubs (*Larrea tridentata*). The dominant wind in this location during the windy season (February to May) is from the southwest (Dukes *et al.,* 2018). Summer rainfall (June– September) accounts for ~60% of the annual precipitation of ~ 250 mm (Muldavin, 2002).

Experimental setup

One 10 m × 5 m monitoring area established in a burned treatment and in a control treatment (~100 m apart) was oriented perpendicular to the dominant wind direction. A prescribed fire was conducted in the burned treament at the start of the annual windy season, approximately one week prior to the start of this experiment in February 2016 (Dukes *et al.,* 2018). The monitoring areas are characterized by similar soil texture, and topography and were chosen to capture the natural heterogeneity of the landscape, with distinct shrub, grass, and bare soil microsites. Each monitoring area had six well-defined shrub islands and had no detectable signs of animal disturbances.

Wind erosion monitoring

Horizontal mass flux (HMF) of sediments, an indicator of aeolian activity, was estimated using custom-made Modified Wilson and Cooke (MWAC) isokinetic sediment samplers that were placed at the downwind side of each monitoring area (Dukes *et al.,* 2018). Six MWAC samplers were installed in both the burned and control monitoring areas. Each MWAC sampler was equipped with four sediment catchers placed at various heights (nominally 0.1, 0.25, 0.5, 0.85 m) and a pivoting wind vane to direct the catchers parallel to the wind direction. The sediments in the MWAC samplers were collected at the end of the windy season 90 days after the initial installation. The HMF (gm^{-1} day^{-1}) is the major contributor to aeolian sediment redistribution and accounts for more than 95% of the sediment flux occurring up to the 1 m height measured from the soil surface (Li *et al.,* 2007). Using data from the MWAC samplers the time-averaged HMF, *q(z)*, was computed as follows:

$$q(z) = \frac{m}{(t)(A_{MWAC})} \tag{1}$$

where z is the height (m) of the center of the MWAC sampler inlet from the ground, m is the mass of sediment (g) collected by the MWAC samplers, t is the collection interval (days), and A_{MWAC} is the area of the MWAC sampler inlet (2.34×10^{-4} m^2). The empirical formula developed by Shao and Raupach (1992) was used to fit the *q(z)* values:

$$q(z) = c_0 e^{\left(c_1 z^2 + c_2 z\right)} \tag{2}$$

where c_0, c_1, and c_2 are fitting constants. The total HMF (Q) was obtained from the integral of *q(z)* from the ground to a height of 1 m (Li *et al.,* 2007; Dukes *et al.,* 2018).

$$Q = \int_0^1 q(z)dz \tag{3}$$

Magnetic tracer

We used two widely used hydrogen-reduced pure solid iron powders (Chemical Store Inc. NJ, USA), IRON100 (Mesh 100) fine powder and IRON325 (Mesh 325) super fine powder (> 99.5% Fe), as the metal tracers. The IRON100 and IRON325 powders were mixed in the ratio 3:1 to create a tracer applicable to a wide particle-size distribution. In actual application, we then mixed 20 g of metal tracer mixture with 80 g of soil (1:5 ratio of tracer and soil) derived from the field site. The soil samples were collected from shrub vegetated microsites (top 2 cm) and were air-dried and passed through a 2 mm sieve before mixing with the iron powder. At the beginning of the windy season (March), ~100 g of magnetic-soil mixture was then uniformly distributed on the six shrub microsites in the burned and control area in a circular pattern (diameter ~0.5 m) around the base of each shrub.

For our study, we considered the particle density effects on terminal velocities of soil and metal particles (Parsons *et al.,* 1993). For the metal and soil grains to have the same fall velocities, the diameter of the tracer particles must be smaller than the soil particles by a factor equal to the square root of the ratio of their submerged specific weights in the fluid (air) (Parsons *et al.,* 1993). Under these conditions, the redistribution of the metal tracer can be used as a proxy for sediment movement. We used a heuristic approach to relate the granulometric distribution of the resulting magnetic tracer mixture from that of the background sediment collected from the samplers from the study area. Background information on the size distribution of the soil and typical sediment particles collected from the site was used to determine the median size of the metal tracer mixture (Ravi *et al.*, 2009b; Gonzales *et al.,* 2018). A comparison of the particle size distribution (PSD) of the tracer mixture (corrected to equivalent aerodynamic diameter of soil grains) with actual PSD of sediments collected using MWAC samplers (0.10 cm) from the study sites indicated that our approach was successful in creating a tracer mixture with similar median diameters (Figure 1). The PSD of the dominant particle sizes emitted from our field sites were the basis for converting the actual iron powder PSD to an equivalent PSD similar to that of the background soil (Hinds, 1999). The size distribution statistics of the tracer mixture can be converted to corresponding aerodynamic equivalent diameters of the sediment particles using Stokes Law. Hence, we assumed that the depletion of iron powder will be proportional to the depletion of normal background sediment as wind erosion occurs (Figure 1). The PSD was determined using a Beckman Coulter LS 13 320 Particle Size Analyzer (LS13320 with aqueous liquid module, Beckman Coulter, Inc., CA, USA), with a dynamic measurement range of 0.017 to 2000 µm.

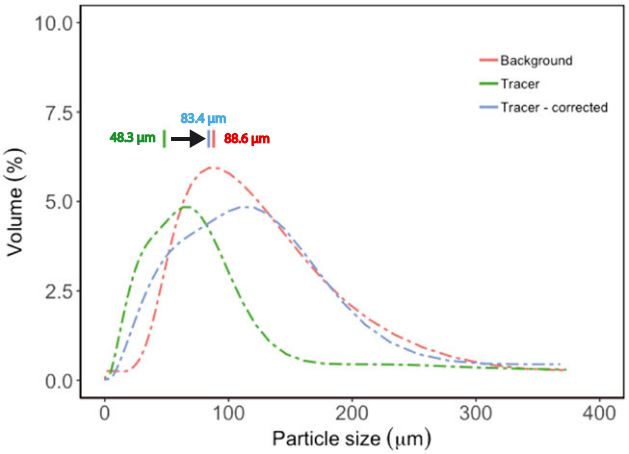

Figure 1. Particle-size distributions (PSD) and median diameters of the tracer, the density corrected tracer, and the aeolian sediments in the background horizontal flux from the study site. [Colour figure can be viewed at wileyonlinelibrary.com]

The spatial changes in low-field magnetic susceptibility at the field site were measured using a magnetic susceptibility meter (Model MS2 Magnetic Susceptibility Meter with an MS2K sensor, Bartington Instruments, Oxfordshire, UK). We measured the bulk magnetic susceptibility (*k*) at 1 m spatial resolution in the 10 m × 5 m plots using a 1 m^2 grid system. The MS measurements were conducted immediately after the application of the tracer at the beginning of the windy season (March, 2016) and at the end of the windy season (June 2016, respectively). To correlate changes in magnetic susceptibility to depletion of soil, the relationship between the fraction of iron tracer in the soil and magnetic susceptibility was determined in the laboratory by using varying concentrations of iron powder tracer (Figure 2). We found a strong linear relationship between iron fraction in the soil and MS values in our measurement range (Figure 2).

Statistical methods

One-way ANOVA with interaction effects was used to test significance of the differences in the horizontal mass flux from the burned and control sites, and between the magnetic susceptibility of soils in the shrub, grass and bare interspace microsites. Semivariance of MS measurements was determined at separation distances of 1–6 m for the burned and control treatments to characterize the relative spatial dependence, or autocorrelation, of spatial patterns of magnetic susceptibility. All statistical analyses were carried out in R (v. 3.4.4, 2018).

Results

Mean and standard deviation of the total HMF (Q) of the control and burned plots were 26.70 ± 2.90 and 47.39 ± 12.60 g m^{-1} d^{-1}, respectively (Figure 3). Thus, the mean Q for the burned plot was 1.8 times greater than that of the control plot during the windy season. One-way ANOVA indicated that

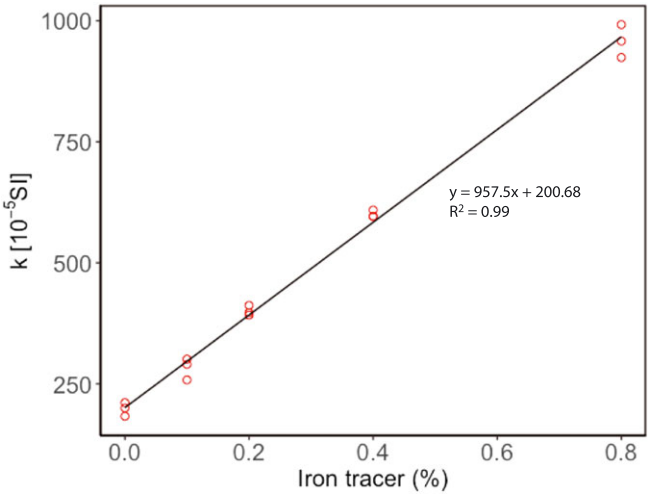

Figure 2. Variation in magnetic susceptibility (MS) with increasing concentration of iron powder tracer in soil samples. [Colour figure can be viewed at wileyonlinelibrary.com]

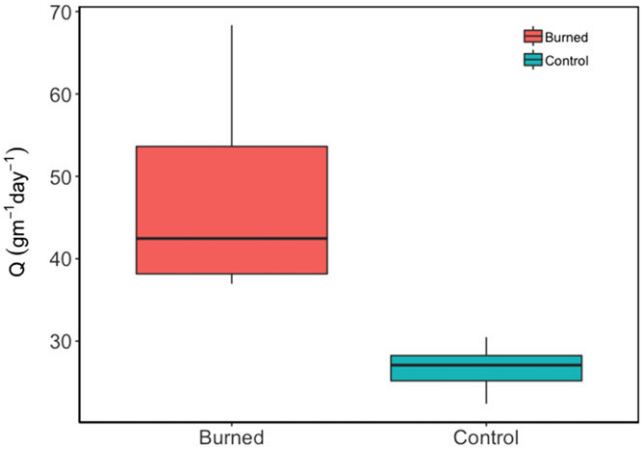

Figure 3. Horizontal mass flux (*Q*) derived from MWAC sediment samplers in the control and burned areas. Q differed significantly between the treatments (one-way ANOVA, $P<0.05$). [Colour figure can be viewed at wileyonlinelibrary.com]

Q differed significantly between the treatments ($F=15.36$, $P<0.005$).

The spatial variation in magnetic susceptibilities for the control and burned areas before and after the windy season are summarized in Figure 4. The magnetic susceptibilities of the shrub microsites decreased to a greater extent in the burned areas after the windy season compared with those in the control areas (Figure 4).

The microsite scale measurements show significant variation in magnetic susceptibility for burned and unburned areas after the tracer was applied to the shrub microsites (Figure 5). Magnetic susceptibility varied significantly between shrub, grass and bare microsites in the control ($F=130.06$, $P<0.005$) and burned ($F=59.58$, $P<0.005$) treatments at the beginning of the windy season (i.e. Day 0, Figure 5). By the end of the windy season in the burned treatment, the magnetic susceptibility decreased for shrub microsites and increased on grass and bare microsites (Figure 5). Significant differences between magnetic susceptibility for each microsite type were observed in the burned area ($F=9.74$, $P<0.005$), but not in the control area ($F=0.06$, $P=0.80$) (Figure 5). Spatial analysis (Figure 6) confirmed that the semivariance of magnetic susceptibility was comparatively low at all separation distances for the burned treatment at the end of the windy season, and thus was more spatially homogenous compared with the beginning of the windy season and compared with the control treatment.

Discussion

In this study, we evaluated a novel affordable metal magnetic susceptibility tracer method in the context of a post-fire wind erosion experiment. Wind erosion, or aeolian sediment transport, has been shown by previous studies in a variety of environments to be elevated following wildfire due to fire-induced removal of vegetation and associated changes in near-surface soil properties (Debano, 2000; Whicker *et al.,* 2002; Ravi, 2009a; Sankey *et al.,* 2009, 2012b, 2012c; Ravi *et al.,* 2012; Stout, 2012). Similarly, in the present experiment, we measured significantly higher horizontal sediment mass flux in a burned compared with a control treatment during a post-fire windy season. Specifically in some shrub–grass ecosystems, aeolian transport following a disturbance occurs along well-defined source to sink pathways that redistribute sediment from burned shrub to grass and bare microsites (White *et al.,* 2006; Sankey *et al.,* 2012a, 2012b ; Dukes *et al.,* 2018 ; Wang *et al.,* 2018). This pattern of post-burn sediment redistribution has been

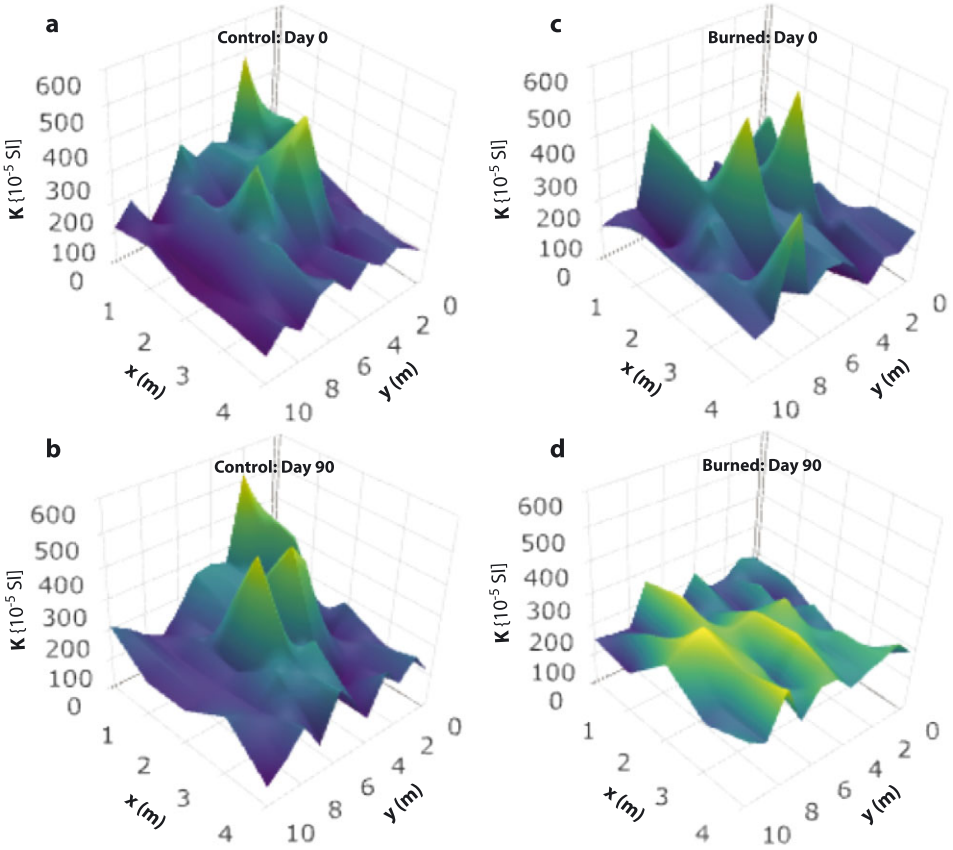

Figure 4. Magnetic susceptibility *k* of control (a, b) and burned (c, d) areas before and 90 days after the prescribed fire respectively. [Colour figure can be viewed at wileyonlinelibrary.com]

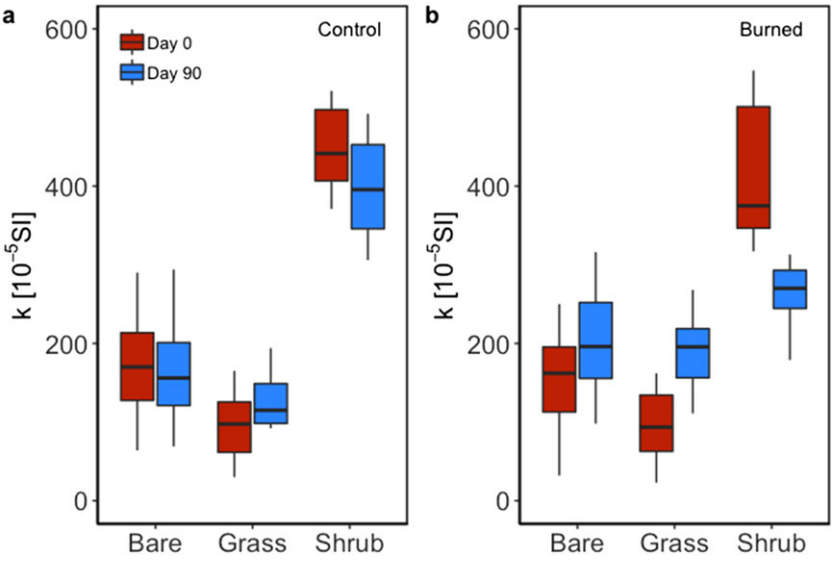

Figure 5. Magnetic susceptibility of vegetation microsites in (a) control and (b) burned areas at the beginning (day 0) and end (day 90) of the windy season. [Colour figure can be viewed at wileyonlinelibrary.com]

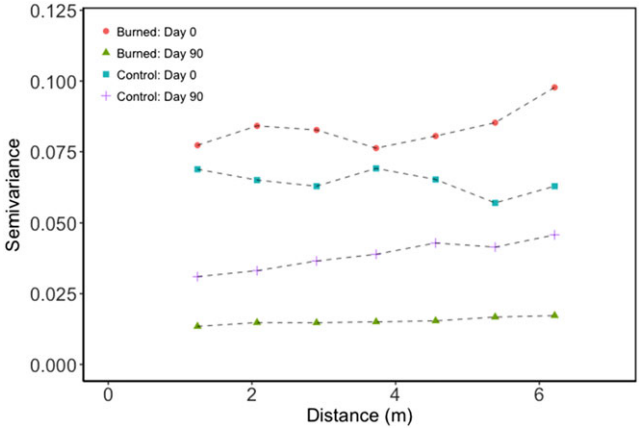

Figure 6. Semivariance of magnetic susceptibility measured on control and burned treatments at the beginning and end of the windy season. [Colour figure can be viewed at wileyonlinelibrary.com]

suggested to distribute soil nutrients more evenly across the landscape and to enhance grass recovery (White *et al.,* 2006; Sankey *et al.,* 2012a, 2012b; Dukes *et al.,* 2018; Wang *et al.,* 2018). In this experiment, we found support for this sediment redistribution pattern in a shrub-grass ecotone using the novel cost-effective tracer method based on magnetic susceptibility.

Results of our study suggest that the burned shrub microsites functioned as a sediment source and the burned grass microsites as a sediment sink during the post-fire windy season. We detected a depletion of the metal tracer in shrub microsites and an enrichment in grass microsites in the burned treatment between the beginning and the end of the experiment. At the end of the windy season, the magnetic susceptibility had decreased significantly on the shrub microsites in the burned treatment but did not change appreciably on the control treatment. This suggests that the tracer was winnowed from the burned shrub microsites, whereas the presence of vegetation elements in the control areas dampened the wind shear on the soil surface and thereby reduced soil erosion. The sheltering effect of non-erodible roughness elements such as vegetation is well known to reduce near-surface wind speed and result in trapping of saltating and reptating particles (Hagen, 1996; Okin and Gillette, 2001; Li *et al.,* 2007; Copeland *et al.,* 2009; Gonzales *et al.,* 2018).

Sediment transported from burned shrub microsites to grass and bare microsites following fires creates spatial patterns of microtopography, soil particle-size distribution, and soil nutrients that are more homogeneous (Sankey *et al.,* 2012a, 2012b; Dukes *et al.,* 2018; Wang *et al.,* 2018). Such resource homogenization is suggested to enhance grass regrowth, thus decreasing aeolian transport and associated land degradation (Ravi *et al.,* 2009b). In our study, the bare and grass microsites in the burned area showed an enrichment of the tracer initially applied underneath shrubs. As grasses are generally fire-adapted and typically retain their pedestals with dense fibrous roots, they are more effective in trapping wind-borne sediments (Stout, 2012; Van Pelt *et al.,* 2017). The post-fire recovery of grasses can be much faster compared with shrubs, thereby offering grasses a competitive advantage in trapping aeolian sediment (Parmenter, 2008). The magnetic tracer approach produced results that provide clear inference to the post-burn redistribution of sediment from shrub microsites to interspaces. Using *in situ* bulk magnetic susceptibility of iron tracer as a proxy for sediment erosion, our findings indicate that the deflation rate from shrub microsites increased by a factor of 1.6 after fire while the horizontal mass flux during this windy season increased by a factor of 1.8. As recently demonstrated by Dukes *et al.* (2018) in this same shrub-grass ecotone, most of the enhanced flux is contributed by the shrub microsites, which are transformed into sediment sources following fires.

Potential limitations

We acknowledge that there are several potential limitations to our tracer-based approach that require further investigation. The tracers may not accurately mimic the movement of soil particles due to density effects as we assume a constant density for sediment particles. In a natural setting, the sediment flux often consists of particles with varying sizes and densities. Moreover, tracer and tracer–soil mixtures would need to be developed, and hence tested, for specific locations to be useful. Prior information on the particle size characteristics of the typical sediment flux and background soil from the study sites should aid in formulating representative tracer mixtures. Moreover, future work could evaluate whether different proportions of horizontal vs vertical aeolian sediment flux impact the concentration of the tracer and the methodology in general. In

areas with significant moisture inputs from precipitation, the chemical properties, such as oxidation potential, of iron tracers and hence the magnetic susceptibility may be altered in the soil over time (Shankar *et al.,* 1996). Other non-corrosive powders such as steel, might offer better stability of applied tracers in the landscape, and could be tested. Nevertheless, our study represents the first step toward the development of a metal magnetic susceptibility tracer for applied aeolian sediment transport research.

Conclusions

We evaluated a cost-effective tracer technique to monitor post-fire soil redistribution from vegetated microsites, using iron powder and spatio-temporal measurements of magnetic susceptibility. Preliminary tests showed that the method was able to elucidate microsite-scale post-fire changes in sediment sources and sinks in the landscape and resource homogenization in the shrub–grass ecotone that have been previously documented by independent means. Therefore, the tracer method emerges from the experiment as a potentially reliable proxy of aeolian sediment transport that should be further investigated for *in situ* field measurements and analytical comparisons. Future studies could evaluate a suite of alternative metal tracers and attempt to understand the stability of the applied tracer in different soil types and precipitation regimes. The metal tracers may provide a valuable tool for monitoring the ecogeomorphic response of landscapes to changing climate, disturbance, and management scenarios.

Acknowledgements—This research was funded by the US National Science Foundation (NSF) EAR-1451518 for S. Ravi and EAR-1451489 for J. Li. The authors gratefully acknowledge the contributions of Jon Erz and Andy Lopez (FWS, SNWR), and Scott Collins (Sevilleta LTER, New Mexico, USA) for providing access to field and laboratory facilities and technical guidance.

References

An Z, Kukla GJ, Porter SC, Xiao J. 1991. Magnetic susceptibility evidence of monsoon variation on the loess plateau of central China during the last 130 000 years. *Quaternary Research* **36**(1): 29–36.

Bagnold RA. 1941. *The Physics of Blown Sand and Desert Dunes*. Methuen: London.

Bityukova L, Scholger R, Birke M. 1999. Magnetic susceptibility as indicator of environmental pollution of soils in Tallinn. *Physics and Chemistry of the Earth, Part A: Solid Earth and Geodesy* **24**(9): 829–835.

Boyko T, Scholger R, Stanjek H. 2004. Topsoil magnetic susceptibility mapping as a tool for pollution monitoring: repeatability of in situ measurements. *Journal of Applied Geophysics* **55**: 249–259.

Breshears DD, Whicker JJ, Johansen MP, Pinder IIIJE. 2003. Wind and water erosion and transport in semiarid shrubland, grassland, and forest ecosystems: quantifying dominance of horizontal wind-driven transport. *Earth Surface Processes and Landforms* **28**: 1189–1209.

Buynevich IV, Bitinas A, Pupienis D. 2007. Lithological anomalies in a relict coastal dune: geophysical and paleoenvironmental markers. *Geophysical Research Letters* **34**: L09707.

Copeland NS, Sharratt BS, Wu JQ, Foltz RB, Dooley JH. 2009. A woodstrand material for wind erosion control: effects on total sediment loss, PM_{10} vertical flux and PM_{10} loss. *Journal of Environmental Quality* **38**: 139–148.

Debano LF. 2000. The role of fire and soil heating on water repellency in wildland environments: a review. *Journal of Hydrology* **231**: 195–206.

Dukes D, Gonzales HB, Ravi S, Grandstaff DE, Van Pelt RS, Li J, Wang G, Sankey JB. 2018. Quantifying postfire aeolian sediment transport using rare earth element tracers. *Journal of Geophysical Research: Biogeosciences* **123**(1): 288–299. https://doi.org/10.1002/2017JG004284.

Field JP, Belnap J, Breshears DD, Neff JC, Okin GS, Whicker JJ, Painter TH, Ravi S, Reheis MC, Reynolds RL. 2010. The ecology of dust. *Frontiers in Ecology and the Environment* **8**(8): 423–430. https://doi.org/10.1890/090050.

Gillette D, Stockton P. 1989. The effect of nonerodible particles on wind erosion of erodible surfaces. *Journal of Geophysical Research: Atmospheres* **94**(D10): 12885–12893. https://doi.org/10.1029/JD094iD10p12885.

Gonzales HB, Ravi S, Li J, Sankey JB. 2018. Ecohydrological implications of aeolian sediment trapping by sparse vegetation in drylands. *Ecohydrology* **11**(7): https://doi.org/10.1002/eco.1986.

Hagen LJ. 1996. Crop residue effects on aerodynamic processes and wind erosion. *Theoretical and Applied Climatology* **54**: 39–46.

Hanesch M, Scholger R. 2002. Mapping of heavy metal loadings in soils by means of magnetic susceptibility measurements. *Environmental Biology* **42**: 857–870.

Hinds WC. 1999. *Aerosol Technology: Properties, Behavior and Measurement of Airborne Particles*, 2nd edn. Wiley: New York.

Hoffmann V, Knab M, Appel E. 1999. Magnetic susceptibility mapping of roadside pollution. *Journal of Geochemical Exploration* **66**: 313–326.

Kok JF, Parteli EJR, Michaels TI, Karam DB. 2012. The physics of wind-blown sand and dust. *Reports on Progress in Physics* **75**: 106901.

Li J, Okin GS, Alvarez L, Epstein H. 2007. Quantitative effects of vegetation cover on wind erosion and soil nutrient loss in a desert grassland of southern New Mexico, USA. *Biogeochemistry* **85**: 317–332.

Magiera T, Strzyszcz Z, Kapicka A, Petrovsky E. 2006. Discrimination of lithogenic and anthropogenic influences on topsoil magnetic susceptibility in Central Europe. *Geoderma* **130**: 299–311.

Miller ME, Bowker MA, Reynolds RL, Goldstein HL. 2012. Post-fire land treatments and wind erosion – lessons from the Milford Flat Fire, UT. *USA. Aeolian Research* **7**: 29–44.

Muldavin EH. 2002. Some floristic characteristics of the northern Chihuahuan Desert: a search for its northern boundary. *Taxon* **51**(3): 453–462.

Okin GS, Gillette DA. 2001. Distribution of vegetation in wind-dominated landscapes: Implications for wind erosion modeling and landscape processes. *Journal of Geophysical Research* **106**(D9): 9673–9683.

Parmenter RR. 2008. Long-term effects of a summer fire on desert grassland plant demographics in New Mexico. *Rangeland Ecology and Management* **61**(2): 156–168. https://doi.org/10.2111/07-010.1.

Parsons AJ, Wainwright J, Abrahams AD. 1993. Tracing sediment movement in interrill overland flow on a semi-arid grassland hillslope using magnetic susceptibility. *Earth Surface Processes and Landforms* **18**(8): 721–732. https://doi.org/10.1002/esp.3290180806.

Pupienis D, Buynevich IV, Jarmalavičius D, Žilinskas G, Fedorovič J. 2013. Regional distribution of heavy-mineral concentrations along the Curonian Spit coast of Lithuania. *Journal of Coastal Research* **2**: 1844–1849.

Ravi S, Baddock MC, Zobeck TM, Hartman J. 2012. Field evidence for differences in post-fire aeolian transport related to vegetation type in semi-arid grasslands. *Aeolian Research* **7**: 3–10. https://doi.org/10.1016/j.aeolia.2011.12.002.

Ravi S, D'Odorico P, Wang L, White CS, Okin GS, Macko SA, Collins SL. 2009b. Post-fire resource redistribution in desert grasslands: a possible negative feedback on land degradation. *Ecosystems* **12**: 434–444. https://doi.org/10.1007/s10021-009-9233-9.

Ravi S, D'Odorico P, Zobeck TM, Over TM. 2009a. The effect of fire-induced soil hydrophobicity on wind erosion in a semiarid grassland: experimental observations and theoretical framework. *Geomorphology* **105**: 80–86. https://doi.org/10.1016/j.geomorph.2007.12.010.

Ravi S, D'Odorico P, Goudie AS, Thomas AD, Okin GS, Li J, Breshears DD, Field JP, Huxman TE, Van Pelt S, Whicker JJ, Swap RJ, Zobeck TM. 2011. Aeolian processes and the biosphere. *Reviews of Geophysics* **49**: RG3001. https://doi.org/10.1029/2010RG000328.

Sankey JB, Germino MJ, Glenn NF. 2009. Aeolian sediment transport following wildfire in sagebrush steppe. *Journal of Arid Environments* **73**(10): 912–919.

Sankey JB, Germino MJ, Glenn NF. 2012c. Dust supply varies with sagebrush microsites and time since burning in experimental erosion events. *Journal of Geophysical Research: Biogeosciences* **117**(G1): 1–13. https://doi.org/10.1029/2011JG001724.

Sankey JB, Germino MJ, Sankey TT, Hoover AN. 2012b. Fire effects on the spatial patterning of soil properties i sagebrush steppe, USA: a meta-analysis. *International Journal of Wildland Fire* **21**(5): 545–556.

Sankey JB, Ravi S, Wallace CSA, Webb RH, Huxman TE. 2012a. Quantifying soil surface change in degraded drylands: shrub encroachment and effects of fire and vegetation removal in a desert grassland. *Journal of Geophysical Research: Biogeosciences* **117**. https://doi.org/10.1029/2012JG002002.

Shankar R, Thompson R, Prakash TN. 1996. Estimation of heavy and opaque mineral contents of beach and offshore placers using rock magnetic techniques. *Geo-Marine Letters* **16**: 313–318.

Shao Y, Raupach MR. 1992. The overshoot and equilibration of saltation. *Journal of Geophysical Research* **97**: 20 559–20 564.

Sharratt BS, Tatarko J, Abatzoglou JT, Fox FA, Huggins D. 2015. Implications of climate change on wind erosion of agricultural lands in the Columbia plateau. *Weather and Climate Extremes* **10**: 20–31. https://doi.org/10.1016/j.wace.2015.06.001.

Stout JE. 2012. A field study of wind erosion following a grass fire on the Llano Estacado of North America. *Journal of Arid Environments* **82**: 165–174.

Van Pelt RS, Baddock MC, Zobeck TM, D'Odorico P, Ravi S, Bhattachan A. 2017. Total vertical sediment flux and PM10 emissions from disturbed Chihuahuan Desert surfaces. *Geoderma* **293**: 19–25. https://doi.org/10.1016/j.geoderma.2017.01.031.

Van Pelt RS, Barnes MCW, Strack JE. 2018. Using rare earth elements to trace wind-driven dispersion of sediments from a point source. *Aeolian Research* **32**: 35–41. https://doi.org/10.1016/J.AEOLIA.2018.01.004.

Wagenbrenner NS, Germino MJ, Lamb BK, Robichaud PR, Foltz RB. 2013. Wind erosion from a sagebrush steppe burned by wildfire: Measurements of PM_{10} and total horizontal sediment flux. *Aeolian Research* **10**: 25–36.

Wang G, Li J, Ravi S, Dukes D, Gonzales HB, Sankey JB. 2018. Post-fire redistribution of soil carbon and nitrogen at a grassland–shrubland ecotone. *Ecosystems*. https://doi.org/10.1007/s10021-018-0260-2.

Wang G, Li J, Ravi S, Scott Van Pelt R, Costa PJM, Dukes D. 2017. Tracer techniques in aeolian research: approaches, applications, and challenges. *Earth-Science Reviews* **170**: 1–16. https://doi.org/10.1016/j.earscirev.2017.05.001.

Webb NP, Pierre C. 2018. Quantifying anthropogenic dust emissions. *Earth's Future* **6**(2): 286–295 http://doi.org/10.1002/2017EF000766.

Whicker JJ, Breshears DD, Wasiolek PT, Kirchner TB, Tavani RA, Schoep DA, Rodgers JC. 2002. Temporal and spatial variation of episodic wind erosion in unburned and burned semiarid shrubland. *Journal of Environmental Quality* **31**(2): 599–612.

White CS, Pendleton RL, Pendleton BK. 2006. Response of two semiarid grasslands to a second fire application. *Rangeland Ecology and Management* **59**(1): 98–106.

